Title

Expanding Functionality of Recombinant Human Collagen Through Engineered Non-Native Cysteines

Journal

BIOMACROMOLECULES, 15(10)

ISSN

1525-7797

Authors

Que, Richard
Mohraz, Ali
Da Silva, Nancy A
et al.

Publication Date

2014

DOI

10.1021/bm500735d

Peer reviewed

Article

pubs.acs.org/Biomac

Expanding Functionality of Recombinant Human Collagen Through Engineered Non-Native Cysteines

Richard Que,[†] Ali Mohraz,[‡] Nancy A. Da Silva,*[,†,‡] and Szu-Wen Wang*[,†,‡]

[†]Department of Biomedical Engineering and [‡]Department of Chemical Engineering and Materials Science, University of California, Irvine, California 92697, United States

Supporting Information

ABSTRACT: Collagen is the most abundant protein in extracellular matrices and is commonly used as a tissue engineering scaffold. However, collagen and other biopolymers from native sources can exhibit limitations when tuning mechanical and biological properties. Cysteines do not naturally occur within the triple-helical region of any native collagen. We utilized a novel modular synthesis strategy to fabricate variants of recombinant human collagen that contained 2, 4, or 8 non-native cysteines at precisely defined locations within each biopolymer. This bottom-up approach introduced capabilities using sulfhydryl chemistry to form hydrogels and immobilize bioactive factors. Collagen variants retained their triple-helical structure and supported cellular adhesion. Hydrogels were characterized using rheology, and the storage moduli were comparable to fibrillar collagen gels at similar concentrations. Furthermore, the introduced cysteines functioned as anchoring sites, with TGF-β1-conjugated collagens promoting myofibroblast differentiation. This approach demonstrates the feasibility to produce custom-designed collagens with chemical functionality not available from native sources.

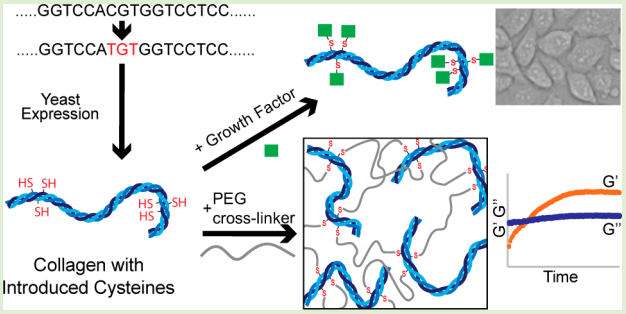

1. INTRODUCTION

The environment that a cell inhabits plays a major role in determining cell fate. Mechanical properties, degradation characteristics, cell-interaction sites, and signaling factor densities of the extracellular matrix (ECM) environment have been shown to modulate proliferation, migration, and differentiation of the residing cells.[1−4] Therefore, components of the ECM, such as the protein collagen, are natural departure points for designing cell substrates and microenvironments in tissue engineering and regenerative medicine. Ideally, biomimetic materials would have the additional advantage over native ECM materials of being amenable to independent control over properties such as protein concentrations, mechanical properties, and densities of cell-interaction sites.[3] Furthermore, engineered materials would not suffer from the typical concerns for materials from animal sources (e.g., batch-to-batch variability, immunogenicity, pathogen transmission).[5−7] Examples of peptides or polymers used as artificial matrices have included hyaluronic acid, fibrinogen, elastin, and the entirely synthetic polymer polyethylene glycol,[8−12] but none are as prevalent in native ECM as the protein collagen.

However, despite collagen being the major component of the ECM, and despite the corresponding high interest to engineer it, efforts to produce collagen synthetically as a matrix backbone have been complicated by challenging issues.[13,14] Collagen's glycine-X-Y tripeptide repeating sequence, together with the unique sequences embedded within the tripeptide repeats required for cell interaction sites, and the large overall number of amino acids, result in difficulties in generating an encoding synthetic gene due to oligonucleotide mishybridizations.[15] Furthermore, prolines in the Y position must be post-translationally hydroxylated for sufficient thermostability of the collagen triple helix.[16] These difficulties have limited most collagen-mimetic materials to short peptides[13,17−21] or repeating collagen-like domains.[22]

Our research group has developed a bottom-up strategy to produce full-length, hydroxylated recombinant collagen III with the native human sequence (rCol) or with alternatively defined sequences. Collagen III, one of the fibrillar collagens, is located in elastic tissues such as the skin, vasculature, and other tissues alongside collagen I.[23,24] It is a homotrimer and expressed from a single gene; therefore, this was selected as our collagen scaffold because it minimizes the number of genes requiring modification to introduce non-native elements into the collagen biopolymer. To overcome the mishybridization problem between oligonucleotides during gene synthesis, the DNA sequence was optimized utilizing an algorithm that considered the degeneracy of the genetic code and oligonucleotide hybridization melting temperatures.[15] Gene synthesis was then performed in modules via PCR assembly. The protein is produced in *Saccharomyces cerevisiae* that has been genetically engineered with the ability to hydroxylate prolines in the

Received: May 22, 2014
Revised: July 24, 2014
Published: August 21, 2014

   dx.doi.org/10.1021/bm500735d | *Biomacromolecules* 2014, 15, 3540−3549

A

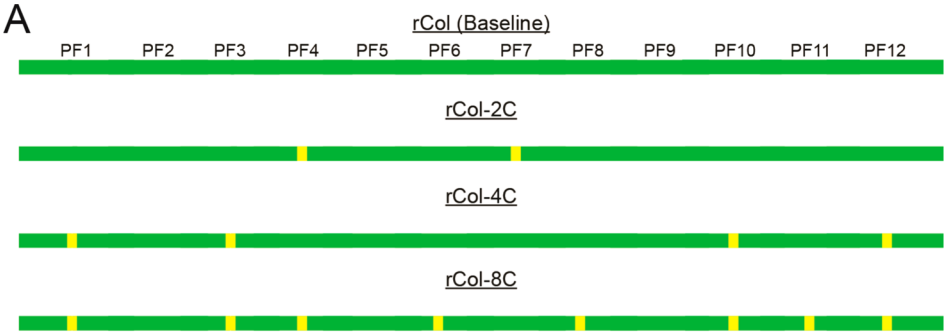

B

Variant	Amino Acid Location Number of Cysteines
rCol	none
rCol-2C	285 (PF4), 731 (PF7)
rCol-4C	42 (PF1), 224 (PF3), 803 (PF10), 984 (PF12)
rCol-8C	42 (PF1), 224 (PF3), 285 (PF4), 465 (PF6), 748(PF8), 803 (PF10), 888 (PF11), 984 (PF12)

Figure 1. Summary of recombinant collagen variants containing non-native cysteines (Cys) in the triple-helical domain. (A) Variants were produced containing 2 to 8 Cys (yellow) spread throughout the triple-helical domain. Green regions denote native amino acid sequences of human collagen III. "PF" indicates the primary fragment (one of 12 modules used in gene synthesis). (B) Collagen variants with the respective amino acid site number of the introduced cysteines.

correct positions within collagen.[25] This strategy provides complete control of the amino acid sequence and allows for the tailoring of sequence, location, and frequency of functional sites within the protein. Our previous work has shown that recombinant human collagen III produced by this platform yields stable triple-helical collagen with correct structure, and this collagen interacts favorably with mammalian cells.[25]

In this study, we examined the feasibility of using our platform to fabricate custom-designed collagen variants. We introduced non-native elements into the human collagen III scaffold, and then probed the structural effects and the functionality of these modified sites. Varying numbers of cysteines (Cys), which are not present in the triple-helical regions of any fibrillar collagen, were inserted at specific sites to be used as cross-linking or attachment sites for bioactive proteins. Although lysines are often used to chemically functionalize collagen from native sources, there are 38 lysines present in the triple-helical region of collagen III,[26] resulting in difficulty in controlling the location and quantity of any lysine-based reactions. In contrast, the exact numbers and locations of Cys sites can be precisely controlled using our platform.

We then examined whether the specifically designed collagens are functional for cross-linking and attachment of bioactive molecules. The sulfhydryl group on Cys is available for reacting with maleimide to form a thioether linkage. One advantage of this approach is to avoid the cytotoxicity of cross-linking lysine amines using either glutaraldehyde or *N*-(3-(dimethylamino)propyl)-*N*′-ethylcarbodiimide (EDC).[27,28] Furthermore, the use of lysines as cross-linking or attachment sites may alter ligand availability as they are contained in binding sequences.[29] These cysteine variants allow for the formation of cross-linked collagen hydrogels with the potential of decoupling stiffness from protein concentration through the control of cysteine density, and thus cross-linking density, per collagen. To examine the feasibility of modulating cell fate through differentiation of fibroblasts to myofibroblasts,[30−32] we immobilized transforming growth factor beta 1 (TGF-β) onto the non-native Cys residues of recombinant collagen variants.

The results of our study demonstrate the ability to produce engineered recombinant collagen with tunability of both physical and biological properties. This approach enables design flexibility of the most prevalent yet synthesis-elusive ECM biopolymer, and it is a significant step toward bottom-up fabrication of artificial cellular microenvironments for tissue engineering.

2. MATERIALS AND METHODS

2.1. Cells and Reagents. *Escherichia coli* DH5α was purchased from Strategene (La Jolla, CA). Restriction endonucleases, DNase I, and RNase I_f were acquired from New England Biolabs (Ipswitch, MA). Phenylmethanesulfonyl fluoride (PMSF), tris(2-carboxyethyl)phosphine (TCEP), bovine serum albumin (BSA), galactose, 40 kDa MWCO desalting columns, methyl-PEG_{24}-NHS [ms$(PEG)_{24}$], and succinimidyl 4-[*N*-maleimidomethyl]cyclohexane-1-carboxylate (SMCC) were obtained from Thermo Fisher (Waltham, MA). Pepsin was purchased from MP Biomedicals (Santa Ana, CA). TGF-β1 was obtained from R&D Systems (Minneapolis, MN). The cross-linking reagent 20 kDa 4-arm PEG maleimide was purchased from NANOCS (Boston, MA). Acrylamide solution was acquired from Bio-Rad (Hercules, CA). Native collagen proteins used as controls were obtained from Millipore (Billerica, MA). Dulbecco's modified Eagle's medium (DMEM), CelLytic M, and monocolonal antibodies against α-smooth muscle actin were purchased from Sigma (St. Louis, MO). Fetal bovine serum (FBS), penicillin, streptomycin, 3-(4,5-dimethylthiazol-2-yl)-2,5-diphenyltetrazolium bromide (MTT), Alexa Fluor 532 C_5-maleimide (AF532), and secondary antibody alkaline phosphatase conjugated antimouse IgG antibodies were obtained from Life Technologies (Carlsbad, CA). Casamino acids, yeast nitrogen base, and tissue culture plates were purchased from BD Biosciences (Franklin Lakes, NJ). NIH/3T3 mouse fibroblast cells and HT-1080 human fibrosarcoma cells were obtained from ATCC (Manassas, VA). Cells were maintained in DMEM supplemented with 10% FBS, 100 U/mL penicillin, and 100 μg/mL streptomycin at 37 °C and 5% CO_2.

2.2. Fabrication of Genes Encoding Collagen Variants. Full length collagen-mimetic proteins were fabricated using the

dx.doi.org/10.1021/bm500735d | *Biomacromolecules* 2014, 15, 3540−3549

modular gene assembly strategy described in Chan et al. to produce recombinant human collagen.[15] The triple-helical region of collagen, for which the gene has been conventionally difficult to assemble, was divided into 12 modules to facilitate synthesis and sequence design. By utilizing the degeneracy of the genetic code, oligonucleotide sequences were optimized to yield higher melting temperatures for correct hybridizations than for incorrect hybridizations.[33] These oligonucleotides were assembled into 12 primary fragments by polymerase chain reaction (PCR). These primary fragments were then PCR-assembled into secondary fragments, and the secondary fragments were PCR-assembled into the full length gene. We showed that this process enables the fabrication of genes encoding the amino acid sequence of human collagen III (which is defined here as "baseline" collagen, rCol) and variants of collagen with desired modulated sequences.[15]

To produce genes coding for collagen containing varying numbers of non-native cysteines, site-directed mutagenesis (SDM) was performed on eight of the 12 primary fragments of the baseline collagen gene to build a library of primary fragments containing one Cys per fragment (see Figure 1). Complementary mutagenic primers used in SDM were designed to change an amino acid of similar size to cysteine in the X or Y position of the Gly-X-Y tripeptide near the center of each primary fragment. This assisted the assembly of primary fragments with and without these non-native cysteines. The mutagenesis procedure was based on protocols described previously,[15] and details are described in the Supporting Information. Briefly, plasmids containing the primary fragments of the baseline human collagen were amplified with their corresponding mutagenic primer pairs in a PCR reaction and digested with *Dpn*I. The DNA product of expected size was transformed into *Escherichia coli* DH5α, and plasmid DNA from colonies grown on LB-Kanamycin were sequenced to confirm the introduction of the Cys mutations and the correct primary fragment sequence.

Primary fragments with and without Cys were mixed-and-matched to assemble secondary fragments with Cys in the desired locations following previously reported protocols;[15] details are provided in Supporting Information. Full length collagen variant genes were assembled from the secondary fragments and sequenced to confirm the correct product. These full length collagen variant genes were then transferred to a *S. cerevisiae* CEN/ARS plasmid as previously described[34] to generate the vectors used for biopolymer expression in yeast. These resulting plasmids are YCpMCOL-2C, YCpMCOL-4C, and YCpMCOL-8C, which contain collagen genes encoding 2, 4, and 8 non-native cysteines, respectively, at roughly equidistant locations along the full-length polymer. Figure 1 summarizes the collagen variants and their corresponding Cys mutations that are encoded by these genes.

2.3. Protein Expression and Purification. Full length recombinant biomimetic collagens were expressed in *S. cerevisiae* BYα2β2, which was engineered to contain two integrated copies each of the human prolyl-4-hydroxylase α-subunit and β-subunit genes to achieve hydroxylation of prolines in the collagen biopolymers.[25] BYα2β2 was transformed with plasmids YCpMCOL-2C, YCpMCOL-4C, and YCpMCOL-8C to express collagen containing 2 Cys [named rCol-2C(1)], 4 Cys [rCol-4C(1)], and 8 Cys [rCol-8C(1)], respectively. In this manuscript, these mutants will be abbreviated as rCol-2C, rCol-4C, and rCol-8C.

To express the recombinant collagen, the yeast were cultured in selective media as previously described,[25] resuspended to 0.1 g/L in ice-cold buffer containing 0.1 M Tris-HCl, 0.4 M NaCl, 2 U/mL DNase, 1 U/mL RNase, and 1 mM PMSF (pH 7.5), and mechanically lysed using a French press cell disruptor (Thermo Fisher, Waltham, MA). EDTA and TCEP were added to the solutions to 1 mM each, and the solutions were incubated for 1 h at 4 °C. The pH was lowered to 2, and the samples were digested with pepsin at a concentration of 0.2 mg/mL for 12 h at 4 °C, conditions which degrade endogenous yeast proteins while leaving hydroxylated triple-helical collagen intact. The digested lysate was cleared by centrifugation. Protein was precipitated from the cleared supernatant by adding acetic acid (HAc) and NaCl to final concentrations of 0.5 M and 3M, respectively, and centrifuged. The precipitate was dissolved in 0.1 N HCl, the solution was raised to pH 7.4 with 200 mM Tris-HCl (pH 8.6), and TCEP was added to 1 mM. After incubation at 4 °C for 1 h, the collagen was precipitated by adding NaCl to 3 M. The pellet was dissolved in 0.1 N HCl and dialyzed against 0.05 M HAc. Protein concentration was determined by BCA assay (Pierce, Rockford, IL) using bovine collagen type III as a standard. SDS-PAGE confirmed size and purity of proteins.

2.4. Characterization of Recombinant Collagen Variants. *Circular Dichroism.* To determine the structure and melting temperatures of the collagen variants, circular dichroism (CD) spectroscopy was performed using a Jasco (Easton, MD) J-810 spectropolarimeter.[35] The purified recombinant collagen samples (100−300 μg/mL) in 50 mM acetic acid were placed in a 1 mm quartz cell and scanned at 10 nm/min. To determine the apparent melting temperature (T_m), the temperature was increased at a rate of 1 °C/min while measuring ellipticity at 221 nm. The molar ellipticity vs temperature was fit to the Gibbs−Helmholtz equation.[36]

Cellular Adhesion. To assess whether the introduced cysteines affected cell adhesion, an adhesion assay was performed as previously described with the recombinant collagens and controls (human collagen III; BSA).[25] Briefly, wells in 96-well, untreated polystyrene plates were coated with 40 μL of 20 μg/mL protein in phosphate buffered saline (PBS, pH 7.4) overnight at 4 °C, and then blocked with 1% BSA in DMEM for 1 h at room temperature (RT, approximately 22 °C). To verify that comparable amounts of protein were deposited between different samples, an alkaline phosphatase assay was performed as previously described.[25] HT-1080 cells were seeded at 1.5 × 10^5 cells/cm^2 in FBS-free DMEM supplemented with 0.1% BSA and incubated at 30 °C for 4 h. Cells were washed with DMEM, incubated with DMEM + 10% FBS for 1 h at 37 °C, and imaged. To quantify the relative number of cells adhered, an MTT assay was used; we incubated cells with 12 mM MTT in DMEM at 37 °C for 2 h, and lysed cells by incubating with 70 μL of 20% w/v sodium dodecyl sulfate, 2 mM HCl, 400 mM HAc in dimethylformamide/water (50:50 v/v) overnight at 37 °C. Absorbance at 570 nm was measured using a SpectraMax M2 plate reader (Molecular Devices, Sunnyvale, CA).

2.5. Functionalization of Collagen through Non-native Cysteines. *Conjugation of Non-native Cysteines with Fluorescent Markers.* To determine the degree of accessibility and chemical functionality of the non-native Cys, the thiol side groups of the Cys were labeled with AF532. Recombinant collagen (1 mg/mL) was incubated with TCEP at a ratio of 2.5 TCEP to 1 Cys in 50 mM phosphate buffer (pH

7) for 30 min at RT, and was then reacted with AF532 (10 AF532 to 1 Cys) for 2 h at RT. As a control, native human collagen was treated with TCEP and AF532 under the same conditions. Unreacted AF532 was removed with a 40 kDa desalting column, and absorbance of the samples was measured at 532 nm. The amount of AF532 within each sample was determined by a standard curve for free AF532. The nonspecific binding of AF532 to the native collagen control was subtracted as the background.

Cross-Linking of Non-native Cysteines to Generate Collagen Hydrogels. The buffer of the different variants of purified collagen was exchanged into 50 mM HEPES (pH 5) at 1 mg/mL protein for passive microrheology, and into PBS (pH 7.4) at 2 mg/mL protein for bulk rheology. TCEP was then added at a ratio of 2.5 TCEP to 1 Cys and incubated at RT for 30 min to reduce any existing disulfide bonds. A 20 kDa, four-arm PEG cross-linker, derivatized with maleimide, was added and mixed at a ratio of 1 maleimide to 1 Cys for microrheology and at a ratio of 2 maleimides to 1 Cys for bulk rheology. Gel formation was characterized by rheological measurements as described below.

Conjugation of Non-native Cysteines with Growth Factor. To examine the effect on cell growth of an immobilized growth factor, TGF-β was attached to rCol-4C. TGF-β was activated with maleimide by reacting it with SMCC (80 SMCC to 1 TGF-β) at RT for 30 min, and excess SMCC was removed using a desalting column. Six-well, untreated polystyrene plates were incubated overnight at 4 °C with 20 μg/mL rCol-4C in PBS. Maleimide-activated TGF-β (50 ng in 1 mL PBS) was reacted with the surface-adsorbed rCol-4C for 2 h at 4 °C. Wells were washed with PBS and incubated with DMEM + 1% BSA for 1 h at RT. These surfaces were then used for subsequent cellular assays.

2.6. Characterization of Cross-Linked Hydrogels. *Passive Microrheology.* To monitor and screen conditions for the formation of a hydrogel from rCol-4C, we used passive multiple particle tracking microrheology.[37] Amine-functionalized polystyrene fluorescent tracer particles of 1 μm diameter were PEGylated with ms$(PEG)_{24}$ to reduce microparticle aggregation. Samples containing collagen protein mixed with cross-linker were prepared as described above at a volume of approximately 10 μL. Fluorescent tracer particles were immediately mixed into the sample after the addition of cross-linker, pipetted between a microscope slide and coverslip separated by 70 μm, and sealed (Norland optical adhesive 81, Norland Products, Cranbury, NJ). Passive microrheology was performed using an Axio Observer inverted microscope (Carl Zeiss Microimaging, Inc., Jena, Germany) attached to a Vt-Eye confocal scanner (VisiTech International, Sunderland, UK). Images were taken at 16 fps for 5 min every hour with a 20x (numerical aperture = 0.4) objective and 2x digital zoom. Samples were monitored over time at RT and the mean square displacement (MSD) of particles was measured by tracking particle centers of mass.[38] Following the method initially outlined by Larsen and Furst, we scaled each individual MSD curve to construct pregel and postgel master curves, and identified the gel point as the transition time between the two curves.[39] To determine the upper limit of elastic modulus measurable with our passive microrheology setup, a control sample of 20% polyacrylamide was prepared from 30% acrylamide/bis-acrylamide (29:1) in a final concentration of 375 mM Tris (pH 8.8), 0.1% w/v APS, 0.1% v/v TEMED.

Bulk Rheology. To confirm the formation of a cross-linked hydrogel using a secondary method and to determine bulk viscoelastic properties of the cross-linked samples, bulk rheology was performed on a stress-controlled rheometer (Anton Paar MCR 301, Graz, Austria) equipped with a 25 mm parallel plate geometry and Peltier temperature control system. Samples containing collagen protein mixed with cross-linker were prepared as described above at a volume of approximately 150 μL and immediately loaded onto the rheometer. A solvent trap filled with ddH_2O was utilized to provide a humidified environment and prevent evaporation from the gel. Oscillatory measurements were performed at a strain of γ = 0.01 and frequency of f = 1 Hz, with a gap height of 200 μm at 22.5 °C. The storage (G') and loss (G'') moduli were recorded over time until G' showed no change over several hours. A frequency sweep was subsequently performed from f = 0.01 to 100 Hz, with all other settings remaining the same.

2.7. Cell Response Assay to Growth Factors Immobilized on Engineered Collagen Substrates. We explored the ability to modulate cellular activity through covalently immobilizing growth factors to recombinant collagen variants. Fibroblast differentiation into myofibroblasts was evaluated by detection of α smooth muscle actin (αSMA) via Western blot.[40] Collagen coated surfaces (rCol, rCol-4C, and native human collagen) incubated with maleimide-functionalized TGF-β in 6-well plates were prepared as described in section 2.5. NIH/3T3 cells were seeded at a density of 6.3×10^4 cells per cm^2 in DMEM + 10% FBS and incubated at 30 °C and 5% CO_2 for 6 h to allow cells to adhere. Wells were washed with PBS, and media was replaced with DMEM + 0.1% FBS. For the controls, collagens that were not mixed with maleimide-functionalized TGF-β were adsorbed to the surfaces, and soluble TGF-β (not maleimide-functionalized) was added to the cell culture media to a final solution concentration of 5 ng/mL (positive controls) or 0 ng/mL (negative controls). Cells were incubated at 30 °C, 5% CO_2 for 48 h then lysed with CelLytic M. Cell lysate was analyzed by Western blot using anti-αSMA primary antibodies raised in mouse and alkaline phosphatase-conjugated rabbit antimouse secondary antibodies. Intensities of bands were quantified using ImageJ software and normalized to the respective positive control (the collagen variant mixed with 5 ng/mL soluble TGF-β) within each blot. Intensity results are reported as mean ± standard deviation and are replicates of four independent experiments.

2.8. Statistical Analysis. For apparent melting temperatures and cell adhesion, results are reported as mean ± standard deviation of at least three independent experiments. Statistical significance was determined using the software program R.[41] We used one-way analysis of variance (ANOVA) followed by the Tukey post-test to evaluate pairwise comparisons. A p-value less than 0.05 was considered significant.

3. RESULTS

3.1. Fabrication and Expression of Cysteine-Containing Collagen Variants. Non-native Cys codons were successfully introduced into primary gene fragments through site-directed mutagenesis, and these gene fragment modules were utilized to assemble the genes encoding full-length collagen variants (Figure 1). Using these genes, the collagen-based proteins rCol-2C, rCol-4C, and rCol-8C, with 2, 4, and 8 Cys per collagen, respectively (corresponding to 6, 12, and 24 Cys per triple-helical polymeric assembly), were successfully

expressed and purified from engineered yeast strain BYα2β2. Approximately 0.5 mg purified protein was recovered per L of culture for rCol-2C and rCol-4C, and approximately 0.05 mg purified protein was recovered per L of culture for rCol-8C. SDS-PAGE analysis showed that the purified rCol-2C and rCol-4C are the expected size, which is consistent with the rCol control (baseline; recombinant human collagen III) and the hCol control (native human collagen III) (Figure 2). These

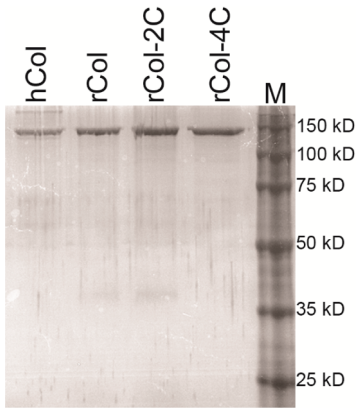

Figure 2. SDS-PAGE of purified collagens and cysteine variants of collagen. Lanes: (1) native human collagen III (hCol); (2) recombinant human collagen III (rCol); (3) recombinant collagen with 2 Cys (rCol-2C); (4) recombinant collagen with 4 Cys (rCol-4C); (5) molecular weight standard (M). The purified recombinant collagens are comparable in size and purity to native human collagen III.

proteins are also as pure and pepsin-resistant as the rCol baseline human collagen. Although rCol-8C was expressed in yeast, purification yields were inconsistent and suggested disulfide cross-linking of the Cys thiols. Therefore, subsequent investigations focused primarily on rCol-2C and rCol-4C.

3.2. Confirmation of Structure, Thermostability, and Cell Adhesion Capability. The structure of the recombinant collagen variants was examined by CD. Variants rCol-2C and rCol-4C were both confirmed to be triple-helical, with the characteristic CD spectra exhibiting a positive peak at 221 nm and negative peak at 198 nm (Figure 3). The thermostability of the triple helix of rCol-2C and rCol-4C were interrogated by CD temperature scans, and yielded apparent melting temperatures (T_m) of 35.9 ± 0.1 °C for rCol-2C and 37.2 ± 0.5 °C for rCol-4C (Figure 3). In comparison, the T_m of recombinant baseline collagen (rCol) is 35.8 ± 0.5 °C.[25] These values for recombinant collagens are all lower than the apparent T_m of 39.1 ± 0.1 °C for native human collagen III ($p < 0.01$). Interestingly, the higher value of T_m for rCol-4C relative to rCol-2C is statistically significant ($p < 0.05$).

We examined whether the introduction of Cys would affect cellular adhesion to the collagen variants. Human collagen III, BSA, rCol, rCol-2C, and rCol-4C were deposited onto surfaces of 96-well plates. Surface protein densities were verified to be equivalent by an ALP-streptavidin−biotin assay. At these experimental conditions, HT-1080 cells adhered to and spread on rCol-2C and rCol-4C substrates at comparable levels as on rCol (baseline) and human collagen III (Figure 4A). In contrast, cells did not adhere to the BSA negative control. These observations were also supported by the quantitative results of the MTT assay (Figure 4B). The numbers of viable cells attached to any of the collagen surfaces were not

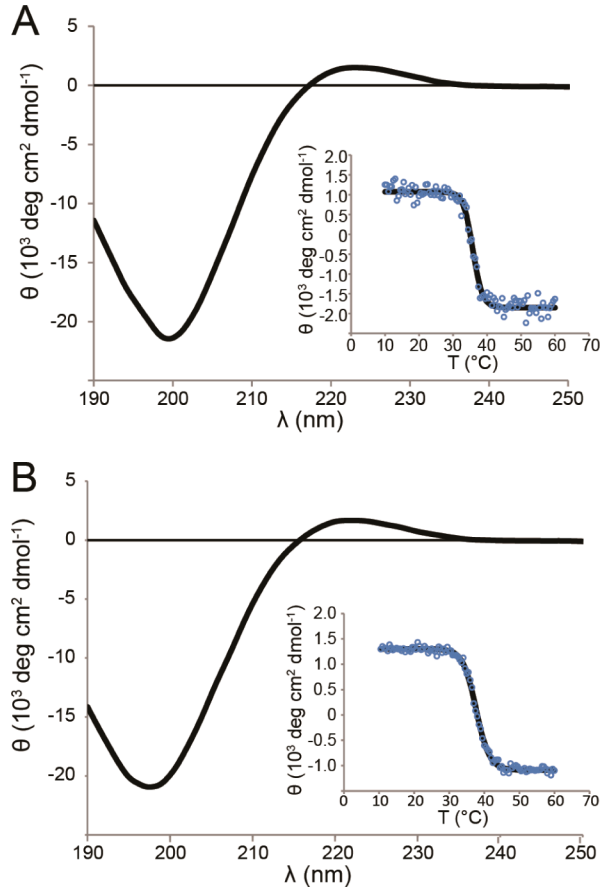

Figure 3. Representative CD data for Cys variants of recombinant collagen. (A) CD wavelength spectra and thermostability scan (inset) for rCol-2C. (B) CD wavelength spectra and thermostability scan (inset) for rCol-4C. Both variants display the characteristic peaks for triple helical collagen and apparent melting temperatures of 35.9 ± 0.1 °C (for rCol-2C) and 37.2 ± 0.5 °C (for rCol-4C).

significantly different from one another, but they were all significantly higher than the number of cells adhered to surfaces coated with the BSA control ($p < 0.001$). Thus, cell adhesion onto recombinant collagen is not inhibited by the introduction of non-native cysteines.

Characterization of rCol-2C and rCol-4C shows that the structure, stability, and cellular adhesion to these variants are similar to those of rCol and to each other. Therefore, we selected the recombinant collagen with the greater number of changes from the baseline, rCol-4C, as the representative variant for subsequent functional characterization.

3.3. Accessibility and Functionality of Non-native Cysteines. *Cysteine Reactions with Small Molecules.* To determine the accessibility and functionality of Cys within our collagen variants, we mixed rCol-4C with a dye molecule that can couple to the Cys thiols. Our results demonstrate that the Cys within rCol-4C is solvent accessible and chemically reactive. The conjugation ratio was determined to be 3.1 ± 0.2 molecules of AF532 to 1 collagen monomer for the given reaction conditions. This corresponds to approximately 77% of the cysteines being labeled.

Formation of Cross-Linked Collagen Hydrogels and Evaluation by Microrheology. To examine whether Cys could be cross-linked for hydrogel formation, rCol-4C was reacted with a maleimide-functionalized PEG cross-linker.

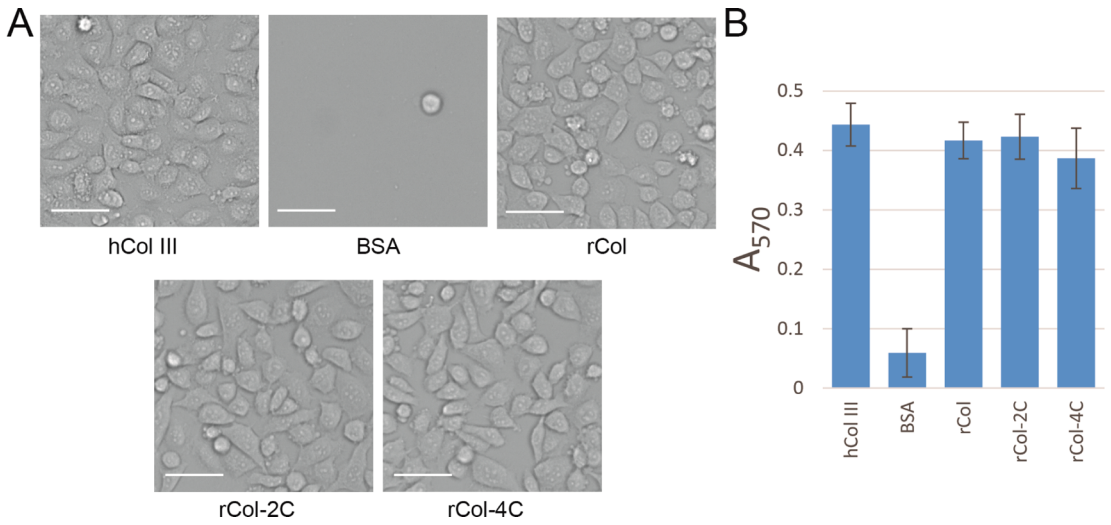

Figure 4. Cell adhesion assays. (A) Images of HT-1080 cells on surfaces adsorbed with native human collagen III (hCol III, positive control), BSA (negative control), baseline recombinant human collagen (rCol), rCol-2C, and rCol-4C. (B) MTT assay to evaluate the relative number of viable cells on these substrates. Cells bind to recombinant collagen containing non-native cysteines. The number of cells adhered to the different collagen surfaces were each significantly greater than the number of cells on BSA ($p < 0.001$), but they were not statistically different from rCol-4C. Scale bar = 50 μm.

Using passive microrheology, we observed that this protein and cross-linker mixture gradually progresses from a viscoelastic liquid to a viscoelastic solid. Tracer particles were tracked over time and the particle MSDs were calculated at various time points. Each MSD curve was scaled utilizing time cure superposition to form the pregel and postgel master curves shown in Figure 5.[39] The MSD of the tracer particles initially

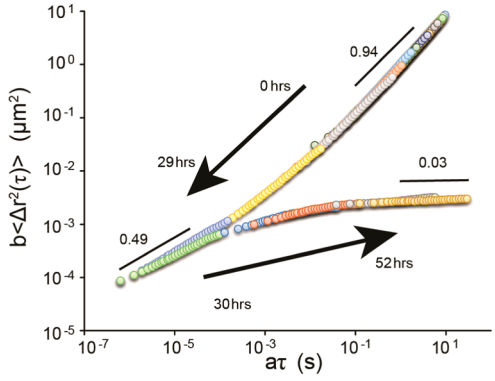

Figure 5. Representative pregel and postgel master curves of cross-linked rCol-4C. Gelation of rCol-4C, cross-linked with maleimide-functionalized PEG, was tracked with passive multiple particle tracking microrheology. Scaled MSD is on the vertical axis and scaled time is on the horizontal axis. Each individual MSD curve taken at different times during gelation is shifted to account for changes in MSD and the relaxation time as cross-links percolate through the sample. Data shows this sample transitioned from a viscoelastic liquid to a viscoelastic solid over time, with gel point time at approximately 29 h.

progressed over time from a slope of near 1 (diffusive dynamics indicative of a liquid-like viscous medium) to the gel point with a slope near 0.5.[42] The postgel master curve shows that samples continued to evolve as the slope of the MSD plot decreases to near 0 (localized dynamics indicative of a solid-like elastic medium) after approximately 50 h. At this point, particles became arrested at the upper limit of stiffness (evaluated here as G' or storage/elastic modulus) distinguishable by our microrheology setup; using a 20% polyacrylamide gel as a standard, this maximum stiffness was determined to be close to 0.3 Pa. Time to gelation varied from approximately 30 to 70 h for identical experimental conditions, demonstrating the kinetics of gelation can vary between replicates. However, the consistent decrease of the MSD slope over time to nearly zero indicates the formation of a cross-linked matrix. The viscoelastic properties of the samples were further evaluated by conventional bulk rheology (see results below). As expected, the recombinant baseline collagen control (no Cys) mixed with cross-linker demonstrated only diffusive behavior with slope near unity in the MSD plot and did not exhibit signatures of gelation up to 15 h; beyond that time point, aggregation of microparticles prevented further measurements.

Formation of Cross-Linked Collagen Hydrogels and Evaluation by Bulk Rheology. After detecting gelation through microrheology, the viscoelastic properties of hydrogels formed from the collagen variants were independently characterized using a conventional rheometer until the storage (G') and loss (G'') moduli remained unchanged over several hours (Figure 6A; Figure S-1, Supporting Information). Samples initially showed more viscous than elastic behavior ($G'' > G'$), but over time became more solid-like ($G' > G''$). The rCol-2C and rCol-4C samples reached the gel point (defined here as the time to reach $G' = G''$), at approximately 2.6 ± 0.4 h and 1.1 ± 0.1 h, respectively. G' values plateaued near 5−10 Pa for rCol-4C after approximately 11.5 ± 1.4 h (Figure 6A). For rCol-2C, G' was 3−4 Pa after approximately 7.6 ± 0.6 h (Figure S-1, Supporting Information). At this point, the storage and loss moduli remained relatively independent of frequency (Figure 6B; Figure S-1); this is characteristic of viscoelastic solids and gel-like materials.[43,44] Recombinant collagen without the introduced non-native cysteines (rCol) was also tested under the same cross-linking conditions as used for rCol-2C and rCol-4C. As expected, the sample remained more viscous than elastic ($G'' > G'$) over the testing period, never reaching a gel point. Collectively, these observations support the formation of a collagen gel through Cys cross-linking.

dx.doi.org/10.1021/bm500735d | *Biomacromolecules* 2014, 15, 3540−3549

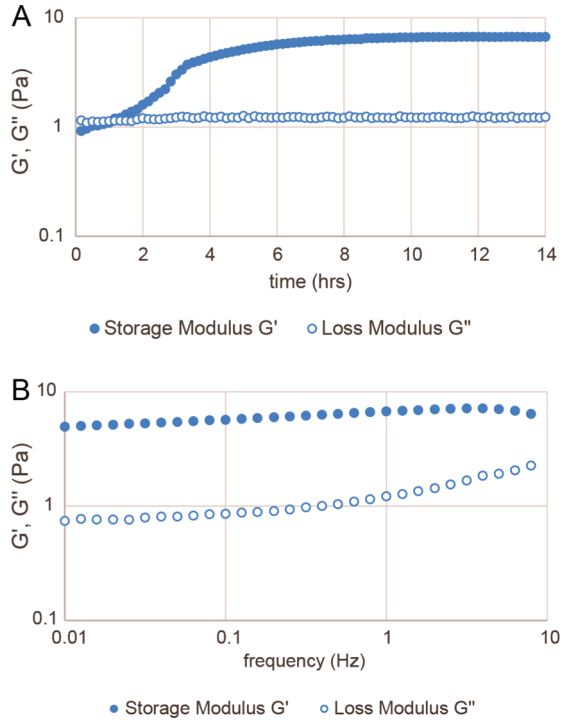

Figure 6. Representative oscillatory rheology data of cross-linked rCol-4C. (A) Storage modulus G' (closed symbols) and loss modulus G'' (open symbols) over time shows transition from liquid-like to solid-like material. (B) Storage modulus G' (closed symbols) is greater than the loss modulus G'' (open symbols) over all frequencies measured for the final solid-like material.

3.4. Cellular Response to Biomimetic Collagen Conjugated with TGF-β. To investigate the feasibility of modulating cellular activity through the covalent conjugation of growth factors, collagen-coated surfaces were reacted with maleimide-activated TGF-β, and NIH/3T3 cells incubated on the coated surfaces were assayed by Western blot for expression of αSMA. The myofibroblast marker, αSMA, was detected in all samples to varying degrees. As expected, the control samples with 5 ng/mL TGF-β in solution (positive controls) exhibited the highest amounts of αSMA, while the samples without TGF-β (negative controls) contained the lowest amounts of αSMA (Figure 7). Importantly, we observed that the band intensity of rCol-4C with TGF-β-maleimide was 1.8 $\pm$ 0.1 times the intensity of rCol (no Cys) with TGF-β-maleimide, highlighting

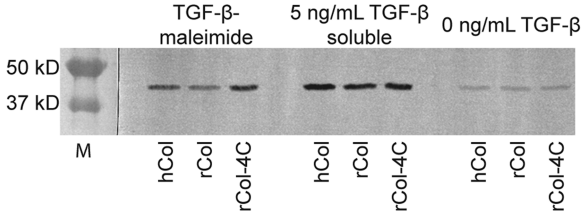

Figure 7. Representative anti-αSMA Western blot of NIH/3T3 cells seeded on different collagen substrates. Lanes: (M) molecular weight markers; (hCol) native human collagen; (rCol) baseline recombinant human collagen; (rCol-4C) recombinant collagen with four Cys per collagen. The first group was treated with maleimide-activated TGF-β and washed with PBS, the second group was treated with TGF-β in solution as a positive control, and the third group was treated with PBS-alone as a negative control.

the effect of covalently immobilizing TGF-β to the Cys collagen variant for promoting myofibroblast differentiation.

4. DISCUSSION

The requirements of the Gly-X-Y peptide repetition, together with the need for unique local sequences embedded within the repeats for cell-recognition sites and a relatively large protein length, makes the collagen gene difficult to synthesize via *de novo* strategies. This synthesis challenge poses a great hurdle to tailoring collagen's protein properties (e.g., tuning scaffold stiffness to guide cell fate or reduce compliance mismatch) to better suit bioengineering applications. Our modular collagen platform is able to address these challenges to yield prescribed, full-length collagen variants. By introducing mutations into the nucleotide sequence of primary fragments, genes encoding different numbers of non-native cysteines were produced by mixing-and-matching primary fragments for PCR assembly. The successful assembly of full-length collagen genes with multiple non-native functional mutations demonstrates the flexibility of the modular collagen platform. If significant changes to the nucleotide sequence are desired, the method of site directed mutagenesis may not suffice, and optimization of the DNA sequence for the desired amino acid sequence and assembly of primary fragments from oligonucleotides may be necessary.[15]

The introduction of four non-native cysteines per molecule, placed in the X or Y position of the Gly-X-Y repeat, did not affect the formation of full-length triple-helical collagen. Although rCol-4C has an approximate 2 °C lower apparent T_m than the value for native human collagen III, it is approximately 1.5 °C higher than that for recombinant baseline collagen III (rCol).[25] Furthermore, rCol-2C retains a similar T_m as rCol. Our yeast expression system has genetically introduced human prolyl-4-hydroxylase to hydroxylate the prolines in collagen. Without the hydroxylase enzymes, the resulting collagen was too unstable to enable purification. The lower apparent T_m of collagen produced by the recombinant yeast system, compared to native human collagen, may be due to differences in proline hydroxylation[25] or lysine hydroxylation, the latter of which increases collagen stability by promoting intramolecular cross-linking between collagen.[45,46] Interestingly, we consistently observe that collagen variants with four Cys (rCol-4C) yield higher T_m values than recombinant rCol without Cys (rCol) or with only two Cys (rCol-2C), potentially due to stabilization from low levels of disulfide cross-linking.

Our prior investigation using atomic force microscopy to examine collagen stability and structure demonstrated that the recombinant collagen retained its triple-helical structure over the time frame of cell adhesion assays when incubated below the T_m.[25] Therefore, to preclude the possibility of thermal denaturation of protein structure in affecting cellular response, cell studies were performed at 30 °C. The thermostability of our recombinant collagens may confine their use to temperatures below 37 °C at this time. To address this possible limitation, we are currently investigating strategies to increase thermostability, including strain engineering (e.g., increasing intracellular ratios of proline hydroxylase to collagen in the yeast) or substrate engineering (e.g., methods to stabilize collagen on solid substrates).

We showed that the introduced cysteines can function as unique and specific cross-linking or attachment sites. Our examination of protein sequences did not identify any cysteines

embedded in the triple-helical fibrillar regions of any collagen from native mammalian sources. Thus, introduction of Cys into the polymeric chain through genetic engineering allows for unique control over the location and the number of the chemically functional thiols in each collagen molecule. Previous studies have introduced sulfhydryls to collagen using Trauts reagent, which reacts with primary amines;[47] however, this strategy does not enable control over the number or locations of reactive sites. This lack of control could potentially lead to heterogeneity of cross-links or immobilized factors, resulting in heterogeneous local properties (e.g., irregular porosity or mechanics, local gradients of growth factor) within the scaffold.

Passive multiparticle microrheology confirmed that our Cys in rCol-4C can be cross-linked to form hydrogels; the material transitioned from a liquid-like to a solid-like character over time as the cross-linking reaction of introduced cysteines with malemide-functionalized PEG proceeded. The resulting collagen reached stiffness values that exceeded the upper sensitivity limit of our passive microrheology setup. Therefore, to gain additional information regarding the viscoelastic properties, we utilized traditional oscillatory rheology. Gelation was also observed, and differences in gel point times between microrheology and bulk rheology may be related to the differences in experimental protocols needed to perform the respective techniques (e.g., pH, presence of PEGylated microparticles), the size of the sample, and variations obtained from probing local versus bulk regions. Particle aggregation that occurred when monitoring rCol samples may have been due to salt bridging between charges on the microparticles and collagen.

One key advantage of using passive microrheology over traditional bulk rheological measurements for artificial ECM studies is the usage of very small sample sizes, which can be beneficial for screening viscoelastic properties of protein-based polymers at different conditions when microbial protein yield is low prior to scale-up. Bulk rheology can subsequently be used to thoroughly examine the variants that are identified to exhibit the desired properties. As our current study has also shown, passive microrheology is limited in the range of measurable parameters, because tracer particle movements are solely driven by thermal energy. A possible alternative technique is active microrheology, which utilizes an external force (e.g., optical or magnetic) to move tracer particles within the material. Active microrheology also requires only small sample quantities, yet potentially provides access to a broader range of measurable rheological parameters compared to passive microrheology.[48]

The storage moduli measured for our cross-linked samples were comparable to those of collagen gels of the same concentration formed through fibril formation,[49,50] and they are also consistent with theoretical estimations based on polymeric lengths and cross-linking densities. Utilizing the equation $G_0 = \nu kT$ where G_0 is the low frequency elastic modulus and ν is the number of polymeric network strands per unit volume,[51] we can estimate the distance between cross-links for our hydrogels to be 100−110 nm for rCol-2C and 70−90 nm for rCol-4C. These numbers are in good agreement with the average distance between the introduced non-native cysteines within each collagen strand, which are approximately 120 nm for rCol-2C and 90 nm for rCol-4C, based on protein sequence. Although the storage modulus or stiffness of the formed gel was relatively low for typical tissue engineering applications, experimental conditions such as the protein concentration, cross-linking ratios, and the length of the cross-linkers could be optimized to obtain the desired viscoelastic properties. For example, studies with recombinant elastin utilize the relatively high concentration of 100 mg/mL to obtain desired mechanical properties.[8] Another study utilizing high molecular weight heparin examined how varying cross-linker length as well as cross-linker ratios can modulate hydrogel stiffness.[42]

We have also shown the ability of the introduced Cys thiols to function as anchoring sites for biofunctional molecules. Tethering of growth factors or other biologically active molecules increases the number and type of tunable parameters in artificial ECM scaffolds. We demonstrated that collagen variants with TGF-β attached to non-native cysteines induced αSMA expression in NIH/3T3 fibroblasts to a greater degree than collagen without the cysteines, supporting a greater extent of myofibroblast differentiation. Other bioactive molecules, such as antibodies for cell capture[47] or VEGF to promote vascularization,[52] could be utilized in lieu of TGF-β to customize the cellular microenvironment.

One limiting constraint of using native ECM sources is the inability to independently control parameters such as protein concentrations, mechanical properties, and densities of cell-reactive sites within collagen.[53] Our platform enables such decoupling in the context of collagen, allowing the determination of the degree to which concentration of collagen, cell signaling site densities, or stiffness of the substrate modulates specific cell behavior. Other hydrogel systems exist that enable this decoupling, but are comprised primarily of the less-abundant ECM proteins (e.g., elastin[54]) or synthetic polymers (e.g., PEG[9]). Collagen mimetic peptides are short building blocks relative to full-length collagen (approximately 10 nm vs 300 nm), and this significantly smaller length can reduce versatility due to available distance for cell activity sites.[55] Though advances have enabled collagen-mimetic peptides to form fibers of 3 to 4 μm in length, these typically involve repeating the same set of peptide sequences in tandem.[56] These alternative strategies rely on identifying specific cell-ECM interactions to engineer the respective known functions. In contrast, our platform utilizes the entire full-length sequence of collagen, which may include uncharacterized epitopes and be beneficial for clinical applications.

5. CONCLUSIONS

In this study, we successfully produced full-length recombinant collagen variants containing non-native cysteines. We demonstrated the functionality of these engineered Cys residues by utilizing them for cross-linking into hydrogels and for growth factor immobilization. The introduction of two or four non-native Cys per collagen monomer (6 or 12 per trimer, respectively) resulted in stable triple helices and supported cell adhesion, both at comparable degrees relative to recombinant collagen without Cys. Thus, this recombinant collagen platform produced unique, specifically prescribed mutants of collagen-mimetic biopolymers, demonstrating proof-of-concept to introduce non-native functional properties into a physiologically important biopolymer.

■ ASSOCIATED CONTENT

Supporting Information

Detailed information on gene synthesis, PEGylation of aminated microparticles, and a representative frequency sweep for collagen variant rCol-2C are presented as Supporting Information. This material is available free of charge via the Internet at http://pubs.acs.org.

AUTHOR INFORMATION

Corresponding Authors

*Mailing address: Department of Chemical Engineering and Materials Science, University of California, Irvine, 916 Engineering Tower, Irvine, CA 92697-2575, USA. Fax: 949-824-2541. E-mail: wangsw@uci.edu, ndasilva@uci.edu.
*E-mail: ndasilva@uci.edu.

Notes

The authors declare no competing financial interest.

ACKNOWLEDGMENTS

We gratefully acknowledge Dr. Hubert Chan for assistance with microrheology and bulk oscillatory rheology, Prof. Eric Weeks for IDL particle tracking scripts, Cory Gierczak for assistance with expression and purification of recombinant collagen protein, and Prof. Eric Furst, Dr. Matthew Shindel, and Dr. Senthil Raman for helpful discussions and initial conditions regarding microrheology. Bulk rheology was performed at the Edwards Lifesciences Center for Advanced Cardiovascular Technology, and CD spectroscopy was performed at the Laser Spectroscopy Facility at UC Irvine. This research was supported by the National Science Foundation (CBET-1034566 and DMR-1006999).

REFERENCES

(1) Davis, G. E.; Senger, D. R. *Circ. Res.* **2005**, *97*, 1093−1107.
(2) Yamamura, N.; Sudo, R.; Ikeda, M.; Tanishita, K. *Tissue Eng.* **2007**, *13*, 1443−1453.
(3) Discher, D. E.; Mooney, D. J.; Zandstra, P. W. *Science* **2009**, *324*, 1673−1677.
(4) Lutolf, M. P.; Hubbell, J. A. *Nat. Biotechnol.* **2005**, *23*, 47−55.
(5) Ruszczak, Z. *Adv. Drug Delivery Rev.* **2003**, *55*, 1595−1611.
(6) Olsen, D.; Yang, C.; Bodo, M.; Chang, R.; Leigh, S.; Baez, J.; Carmichael, D.; Perälä, M.; Hämäläinen, E.-R.; Jarvinen, M.; Polarek, J. *Adv. Drug Delivery Rev.* **2003**, *55*, 1547−1567.
(7) Asher, D. M. *Dev. Biol. Stand.* **1999**, *100*, 103−118.
(8) Straley, K. S.; Heilshorn, S. C. *Soft Matter* **2009**, *5*, 114−124.
(9) Lutolf, M. P.; Lauer-Fields, J. L.; Schmoekel, H. G.; Metters, A. T.; Weber, F. E.; Fields, G. B.; Hubbell, J. A. *Proc. Natl. Acad. Sci. U. S. A.* **2003**, *100*, 5413−5418.
(10) Raeber, G. P.; Lutolf, M. P.; Hubbell, J. A. *Biophys. J.* **2005**, *89*, 1374−1388.
(11) Sengupta, D.; Heilshorn, S. C. *Tissue Eng., Part B: Rev.* **2010**, *16*, 285−293.
(12) Shapira-Schweitzer, K.; Seliktar, D. *Acta Biomater.* **2007**, *3*, 33−41.
(13) Shoulders, M. D.; Raines, R. T. *Annu. Rev. Biochem.* **2009**, *78*, 929−958.
(14) Chattopadhyay, S.; Raines, R. T. *Biopolymers* **2014**, *101*, 821−833.
(15) Chan, S. W. P.; Hung, S.-P.; Raman, S. K.; Hatfield, G. W.; Lathrop, R. H.; Da Silva, N. A.; Wang, S.-W. *Biomacromolecules* **2010**, *11*, 1460−1469.
(16) Szpak, P. *J. Archaeol. Sci.* **2011**, *38*, 3358−3372.
(17) Rubert Pérez, C. M.; Panitch, A.; Chmielewski, J. *Macromol. Biosci.* **2011**, *11*, 1426−1431.
(18) Przybyla, D. E.; Chmielewski, J. *Biochemistry* **2010**, *49*, 4411−4419.
(19) Reyes, C. D.; García, A. J. *J. Biomed. Mater. Res., Part A* **2003**, *65A*, 511−523.
(20) Brodsky, B.; Thiagarajan, G.; Madhan, B.; Kar, K. *Biopolymers* **2008**, *89*, 345−353.
(21) Yu, S. M.; Li, Y.; Kim, D. *Soft Matter* **2011**, *7*, 7927−7938.
(22) Majsterek, I.; McAdams, E.; Adachi, E.; Dhume, S. T.; Fertala, A. *Protein Sci.* **2003**, *12*, 2063−2072.
(23) Royce, P. M.; Steinmann, B. *Connective Tissue and Its Heritable Disorders: Molecular, Genetic, and Medical Aspects*; John Wiley & Sons: Hoboken, NJ, 2003.
(24) Bourhis, J.-M.; Mariano, N.; Zhao, Y.; Harlos, K.; Exposito, J.-Y.; Jones, E. Y.; Moali, C.; Aghajari, N.; Hulmes, D. J. S. *Nat. Struct. Mol. Biol.* **2012**, *19*, 1031−1036.
(25) Jabaiah, A.; Wang, X.; Raman, S. K.; Ragan, R.; Da Silva, N. A.; Wang, S.-W. *J. Biomater. Appl.* **2014**, *28*, 1354−1365.
(26) Strausberg, R. L.; Feingold, E. A.; Grouse, L. H.; Derge, J. G.; Klausner, R. D.; Collins, F. S.; Wagner, L.; Shenmen, C. M.; Schuler, G. D.; Altschul, S. F.; Zeeberg, B.; Buetow, K. H.; Schaefer, C. F.; Bhat, N. K.; Hopkins, R. F.; Jordan, H.; Moore, T.; Max, S. I.; Wang, J.; Hsieh, F.; Diatchenko, L.; Marusina, K.; Farmer, A. A.; Rubin, G. M.; Hong, L.; Stapleton, M.; Soares, M. B.; Bonaldo, M. F.; Casavant, T. L.; Scheetz, T. E.; Brownstein, M. J.; Usdin, T. B.; Toshiyuki, S.; Carninci, P.; Prange, C.; Raha, S. S.; Loquellano, N. A.; Peters, G. J.; Abramson, R. D.; Mullahy, S. J.; Bosak, S. A.; McEwan, P. J.; McKernan, K. J.; Malek, J. A.; Gunaratne, P. H.; Richards, S.; Worley, K. C.; Hale, S.; Garcia, A. M.; Gay, L. J.; Hulyk, S. W.; Villalon, D. K.; Muzny, D. M.; Sodergren, E. J.; Lu, X.; Gibbs, R. A.; Fahey, J.; Helton, E.; Ketteman, M.; Madan, A.; Rodrigues, S.; Sanchez, A.; Whiting, M.; Madan, A.; Young, A. C.; Shevchenko, Y.; Bouffard, G. G.; Blakesley, R. W.; Touchman, J. W.; Green, E. D.; Dickson, M. C.; Rodriguez, A. C.; Grimwood, J.; Schmutz, J.; Myers, R. M.; Butterfield, Y. S. N.; Krzywinski, M. I.; Skalska, U.; Smailus, D. E.; Schnerch, A.; Schein, J. E.; Jones, S. J. M.; Marra, M. A. Mammalian Gene Collection Program Team. *Proc. Natl. Acad. Sci. U. S. A.* **2002**, *99*, 16899−16903.
(27) Moshnikova, A. B.; Afanasyev, V. N.; Proussakova, O. V.; Chernyshov, S.; Gogvadze, V.; Beletsky, I. P. *Cell. Mol. Life Sci. CMLS* **2006**, *63*, 229−234.
(28) Lee, C. R.; Grodzinsky, A. J.; Spector, M. *Biomaterials* **2001**, *22*, 3145−3154.
(29) Trappmann, B.; Chen, C. S. *Curr. Opin. Biotechnol.* **2013**, *24*, 948−953.
(30) Barrientos, S.; Stojadinovic, O.; Golinko, M. S.; Brem, H.; Tomic-Canic, M. *Wound Repair Regen.* **2008**, *16*, 585−601.
(31) Grande, J. P. *Proc. Soc. Exp. Biol. Med.* **1997**, *214*, 27−40.
(32) Montesano, R.; Orci, L. *Proc. Natl. Acad. Sci. U. S. A.* **1988**, *85*, 4894−4897.
(33) Larsen, L. S. Z.; Wassman, C. D.; Hatfield, G. W.; Lathrop, R. H. *Int. J. Bioinf. Res. Appl.* **2008**, *4*, 324−336.
(34) Chan, S. W.; Greaves, J.; Da Silva, N.; Wang, S.-W. *BMC Biotechnol.* **2012**, *12*, 51.
(35) Greenfield, N. J. *Nat. Protoc.* **2007**, *1*, 2876−2890.
(36) Greenfield, N. J. *Nat. Protoc.* **2007**, *1*, 2527−2535.
(37) Mason, T. G.; Weitz, D. A. *Phys. Rev. Lett.* **1995**, *74*, 1250−1253.
(38) Crocker, J. C.; Grier, D. G. *J. Colloid Interface Sci.* **1996**, *179*, 298−310.
(39) Larsen, T. H.; Furst, E. M. *Phys. Rev. Lett.* **2008**, *100*, 146001.
(40) Evans, R. A.; Tian, Y. C.; Steadman, R.; Phillips, A. O. *Exp. Cell Res.* **2003**, *282*, 90−100.
(41) R Core Team. *R: A Language and Environment for Statistical Computing*; R Foundation for Statistical Computing: Vienna, Austria, 2013.
(42) Schultz, K. M.; Baldwin, A. D.; Kiick, K. L.; Furst, E. M. *Macromolecules* **2009**, *42*, 5310−5316.
(43) Winter, H. H.; Chambon, F. *J. Rheol.* **1986**, *30*, 367−382.
(44) Calvet, D.; Wong, J. Y.; Giasson, S. *Macromolecules* **2004**, *37*, 7762−7771.
(45) Jimenez, S.; Harsch, M.; Rosenbloom, J. *Biochem. Biophys. Res. Commun.* **1973**, *52*, 106−114.
(46) Yamauchi, M.; Shiiba, M. In *Post-translational Modifications of Proteins*; Kannicht, C., Ed.; Methods in Molecular Biology; Humana Press: Totowa, NJ, 2008; Vol. *446*, pp 95−108.
(47) Shi, C.; Li, Q.; Zhao, Y.; Chen, W.; Chen, B.; Xiao, Z.; Lin, H.; Nie, L.; Wang, D.; Dai, J. *Biomaterials* **2011**, *32*, 2508−2515.
(48) Sriram, I.; Furst, E. M.; DePuit, R. J.; Squires, T. M. *J. Rheol.* **2009**, *53*, 357−381.

(49) Willits, R. K.; Skornia, S. L. *J. Biomater. Sci. Polym. Ed.* **2004**, *15*, 1521−1531.
(50) Yang, Y.; Leone, L. M.; Kaufman, L. J. *Biophys. J.* **2009**, *97*, 2051−2060.
(51) Larson, R. G. *The Structure and Rheology of Complex Fluids*; Oxford University Press: Oxford, U.K., 1999; p 238.
(52) Shen, Y. H.; Shoichet, M. S.; Radisic, M. *Acta Biomater.* **2008**, *4*, 477−489.
(53) Lampe, K. J.; Heilshorn, S. C. *Neurosci. Lett.* **2012**, *519*, 138−146.
(54) Lampe, K. J.; Antaris, A. L.; Heilshorn, S. C. *Acta Biomater.* **2013**, *9*, 5590−5599.
(55) Kotch, F. W.; Raines, R. T. *Proc. Natl. Acad. Sci. U. S. A.* **2006**, *103*, 3028−3033.
(56) Rele, S.; Song, Y.; Apkarian, R. P.; Qu, Z.; Conticello, V. P.; Chaikof, E. L. *J. Am. Chem. Soc.* **2007**, *129*, 14780−14787.